



Available online at www.sciencedirect.com

ScienceDirect

Procedia Engineering 126 (2015) 716 – 720

**Procedia
Engineering**

www.elsevier.com/locate/procedia

7th International Conference on Fluid Mechanics, ICFM7

Induced pressure fields of power-law fluids electroosmotic flow in micro-diffuser at different angles

Juan Duan, Qing-Yong Zhu*

School of Engineering, Sun Yat-sen University, Guangzhou 510275, China

Abstract

This paper describes the induced pressure of power-law fluids electroosmotic flow (EOF) in micro-diffuser at different angles such as 30° and 60°. Ostwald-De Wael model is used to describe the power-law fluids, and high accuracy compact difference algorithm is used to solve complete Poisson-Boltzmann equations and modified two-dimension Cauchy momentum equations. Poisson equation of pressure is solved by the velocity and pressure method. Dimensionless induced pressure nephogram and mean axial velocity are shown in this study. While the diffuser angles is 30° or 60°, the impact of induced pressure is much more significant than that without pressure gradient. Dimensionless mean velocity profiles with induced pressure have a larger error than the situation without it. Shear thinning fluid is sensitive to the change of flow filed while shear thickening fluid is the opposite. For EOF in variable section, the influence of induced pressure should not be neglected. Especially for less viscous fluid such as shear thinning fluid, it has a larger error with induced pressure compared without it.

© 2015 The Authors. Published by Elsevier Ltd. This is an open access article under the CC BY-NC-ND license (<http://creativecommons.org/licenses/by-nc-nd/4.0/>).

Peer-review under responsibility of The Chinese Society of Theoretical and Applied Mechanics (CSTAM)

Keywords: Induced pressure gradient; Micro-diffuser; Power-law fluids; Electroosmotic flow

1. Introduction

Electroosmotic flow is widely used in microsystem. Many micro devices are designed to have variable section and the micro-diffuser is typical one. Then the fluid flow characteristics in micro-diffuser are the focus of this study.

* Corresponding author. Tel.: +86-020-84036235; fax: +86-020-84036235.
E-mail address: mcszqy@mail.sysu.edu.cn

Non-Newtonian fluids are closer to actual fluids than Newtonian. Power-law fluids satisfied Ostwald-De Wael law electroosmotic flow (EOF) in micro-diffuser are also the study object of this paper.

Pressure gradient is ignored in Navier-Stocks equations in studying the EOF, but flow can induce the pressure gradient. Many researchers studied the EOF velocity profiles without taking account of induced pressure gradient. Tang et al. [1] used the lattice Boltzmann methodology to study the power-law fluids EOF between two parallel plates, but they did not consider how to deal with the pressure gradient and no values for pressure inlet or outlet. Zhao et al. [2] deduced the velocity analytical solutions of power-law fluids electroosmotic flow in parallel-plate microchannel without the pressure gradient. There are also several papers taking the pressure gradient into account. Zhang et al. [3] found that induced pressure gradients could cause band-broadening effects that affect the performance of microfluidic devices. Chen et al. [4] discussed the EOF and particle transport in micro-diffuser and showed the induced pressure and pressure gradient profiles. We are interested in the difference of flow fields with and without the induced pressure gradient. This paper focuses on the impact of induced pressure gradient. The difference of velocity with and without pressure gradient at different diffuser angles are shown. Flow characteristics of shear thinning and thickening fluids are presented in detail, compared to Newtonian counterparts.

Nomenclature

a	hydraulic radius
r_0, R_0	the maximum radius of micro-diffuser in upstream section or downstream section
r, z	dimensionless radius, axial length
L_1, L_2, L_3	lengths of upstream, diffuser and downstream sections, define $L = L_1 + L_2 + L_3$
\bar{v}, u	dimensionless radial velocity, axial velocity
u_s	the Helmholtz-Smoluchowski velocity
\bar{p}	dimensionless pressure
t	dimensionless time
E, E_0	external electric intensity, the maximum external electric intensity
Re_0	Reynolds number
α	diffuser angle of micro-diffuser
κ	Debye-Hückel parameter (m^{-1})
Ψ, Ψ_s	dimensionless electric potential of electric double-layer (EDL), electrical potential on the wall
$\bar{\eta}$	dimensionless apparent viscosity of power-law fluids
μ, μ_0	dynamic viscosity coefficient with dimension [$N \cdot s^a / m^2$], dynamic viscosity coefficient of Newtonian

2. Mathematic model and methods

Fig. 1 shows the micro-diffuser model for numerical simulation. The density of power-law fluids flowing in micro-diffuser is 998 kg/m^3 , and the proportion of positive and negative ions concentration is 1:1.

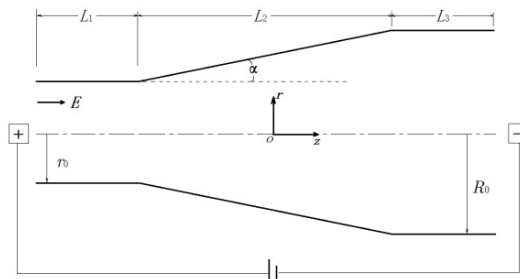


Fig. 1. EOF in micro-diffuser model.

2.1. The complete Poisson-Boltzmann equations

Different electric distribution can induce the different EOF. According to electrostatics theory, we use the Poisson equation and Boltzmann distribution [5] to describe the electric potential distribution in electric double-layer (EDL). The cylindrical coordinate system is used to simplify the three-dimensional equations to two-dimensional equations, and the symmetric cross section is analyzed. Dimensionless two-dimensional Poisson-Boltzmann (P-B) equations and boundary conditions are derived as,

$$\frac{\partial^2 \Psi}{\partial z^2} + \frac{\partial^2 \Psi}{\partial r^2} + \frac{1}{r} \frac{\partial \Psi}{\partial r} = (\kappa a)^2 \sinh(\Psi), \quad (1)$$

$$\begin{cases} \bar{r} = 0, \frac{\partial \Psi}{\partial r} = 0; & \bar{r} = \frac{R}{a}, \Psi = \Psi_s, (r_0 \leq R \leq R_0) \\ \bar{z} = 0, \frac{\partial \Psi}{\partial z} = 0; & \bar{z} = \frac{L}{a}, \frac{\partial \Psi}{\partial z} = 0 \end{cases} \quad (2)$$

2.2. Modified two-dimension Cauchy momentum equations

Modified Cauchy momentum equations [6] are used to describe the flow field. The velocity and pressure methods is used to solve the Poisson equation of pressure. Space terms of Eq. (3) are solved by fourth-order compact finite difference scheme, and third-order Runge-Kutta method is used to solve the time terms. Tthe modified Cauchy momentum equations can be normalized as,

$$\begin{cases} \frac{\partial \bar{v}}{\partial t} + \text{Re}_0 \left(\frac{-\partial \bar{v}}{\partial r} + u \frac{\partial \bar{v}}{\partial z} \right) = -\frac{\partial \bar{p}}{\partial r} + \frac{2\mu}{\mu_0} \left(\frac{u_s}{a} \right)^{n-1} \left[\frac{\bar{\eta}}{r} \frac{\partial \bar{v}}{\partial r} + \frac{\partial}{\partial r} \left(\frac{-\partial \bar{v}}{\partial r} \right) + \frac{1}{2} \frac{\partial}{\partial z} \left(\bar{\eta} \left(\frac{\partial \bar{v}}{\partial z} + \frac{\partial \bar{u}}{\partial r} \right) \right) - \bar{\eta} \frac{\bar{v}}{r} \right] \\ \frac{\partial \bar{u}}{\partial t} + \text{Re}_0 \left(\frac{-\partial \bar{u}}{\partial r} + u \frac{\partial \bar{u}}{\partial z} \right) = -\frac{\partial \bar{p}}{\partial z} + \frac{\mu}{\mu_0} \left(\frac{u_s}{a} \right)^{n-1} \left[\frac{1}{r} \frac{\partial}{\partial r} \left(r \bar{\eta} \left(\frac{\partial \bar{v}}{\partial z} + \frac{\partial \bar{u}}{\partial r} \right) \right) + 2 \frac{\partial}{\partial z} \left(\bar{\eta} \frac{\partial \bar{u}}{\partial z} \right) \right] + \frac{\mu}{\mu_0} \frac{(\kappa a)^2}{E_0 \Psi_s} E \sinh(\Psi), \\ \frac{\partial^2 \bar{p}}{\partial r^2} + \frac{\partial^2 \bar{p}}{\partial z^2} = S_p \end{cases} \quad (3)$$

where S_p is derived as follows,

$$\begin{aligned} S_p = & \frac{2\mu}{\mu_0} \left(\frac{u_s}{a} \right)^{n-1} \left[\frac{\partial}{\partial r} \left(\frac{\bar{\eta}}{r} \frac{\partial \bar{v}}{\partial r} \right) + \frac{\partial^2}{\partial r^2} \left(\frac{-\partial \bar{v}}{\partial r} \right) + \frac{\partial^2}{\partial z^2} \left(\bar{\eta} \frac{\partial \bar{u}}{\partial z} \right) + 2 \frac{\partial^2}{\partial z \partial r} \left(\bar{\eta} \left(\frac{\partial \bar{v}}{\partial z} + \frac{\partial \bar{u}}{\partial r} \right) \right) + \frac{2}{r} \frac{\partial^2}{\partial r \partial z} \left(r \bar{\eta} \left(\frac{\partial \bar{v}}{\partial z} + \frac{\partial \bar{u}}{\partial r} \right) \right) - \frac{\partial}{\partial r} \left(\bar{\eta} \frac{\bar{v}}{r} \right) \right] \\ & - \frac{\partial}{\partial t} \left(\frac{\partial \bar{v}}{\partial r} + \frac{\partial \bar{u}}{\partial z} \right) - \text{Re}_0 \left[\frac{\partial}{\partial r} \left(\frac{-\partial \bar{v}}{\partial r} + u \frac{\partial \bar{v}}{\partial z} \right) + \frac{\partial}{\partial z} \left(\frac{-\partial \bar{u}}{\partial r} + u \frac{\partial \bar{u}}{\partial z} \right) \right] \end{aligned} \quad (4)$$

The initial and boundary conditions of Eq. (3) are as follows,

$$\begin{cases} \bar{t} = 0, \bar{v} = 0, \bar{u} = 0, \bar{p} = 0 \\ \bar{r} = 0, \bar{v} = 0, \frac{\partial \bar{u}}{\partial r} = 0; & \bar{r} = \frac{R}{a}, \bar{v} = 0, \bar{u} = 0, (r_0 \leq R \leq R_0) \\ \bar{z} = 0, \bar{v} = 0, \frac{\partial \bar{u}}{\partial z} = 0, \bar{p} = 0; & \bar{z} = \frac{L}{a}, \bar{v} = 0, \frac{\partial \bar{u}}{\partial z} = 0, \bar{p} = 0 \end{cases} \quad (5)$$

3. Results

Table 1 shows the values of parameters used in calculation. Dimensionless electrokinetic width κa is 32.75 in this paper.

Table 1. Values of parameters.

Parameters	Values	Units
μ_0	9×10^{-4}	$\text{N}\cdot\text{s}/\text{m}^2$
μ	9×10^{-4}	$\text{N}\cdot\text{s}^n/\text{m}^2$
E/E_0	1	-
L_1, L_2, L_3	50	μm
r_0	10	μm

3.1. Dimensionless induced pressure nephogram at steady state

3.1.1. Pressure of power-law fluids at $\alpha = 30^\circ$

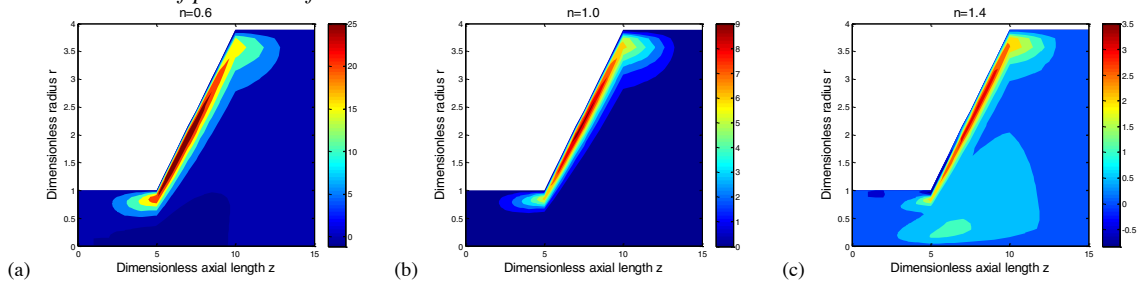


Fig. 2. Induced pressure profiles of power-law fluids at $\alpha = 30^\circ$. (a)Shear thinning fluid; (b)Newtonian; (c)Shear thickening fluid.

3.1.2. Pressure of power-law fluids at $\alpha = 60^\circ$

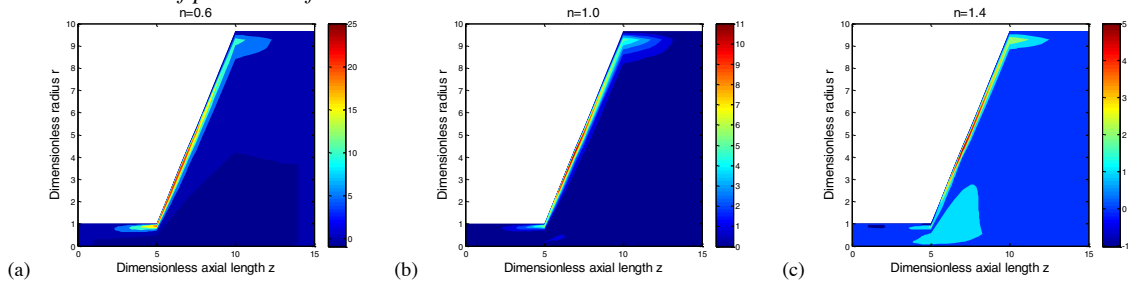


Fig. 3. Induced pressure profiles of power-law fluids at $\alpha = 60^\circ$. (a)Shear thinning fluid; (b)Newtonian; (c)Shear thickening fluid.

Figs. 2 and 3 show that the pressure is high near the wall especially in diffuser zone and pressure gradient is large axially. Shear thinning fluid owns the largest pressure gradient.

3.2. Dimensionless mean axial velocity profiles at steady state

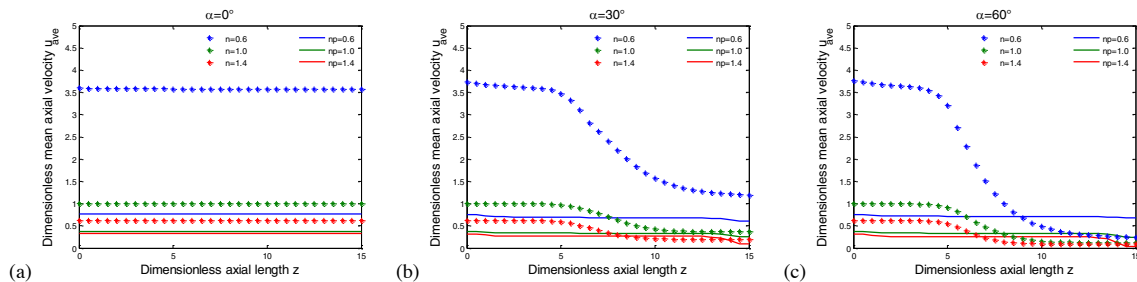


Fig. 4. Comparison of dimensionless mean velocity of power-law fluids with induced pressure and without it in steady state at different diffuser angles. (a) $\alpha = 0^\circ$; (b) $\alpha = 30^\circ$; (c) $\alpha = 60^\circ$. In figures the n is stand for velocity without induced pressure gradient and the np is opposite.

Fig. 4 shows that the dimensionless mean axial velocity of power-law fluids with pressure gradient are compared to that without pressure gradient at the steady state. And the errors are so large that we cannot neglect the influence of induced pressure gradient no matter what the diffuser angle is 0° , 30° or 60° . While taking the induced pressure gradient into account, trend of mean velocity changes gently and the diffuser angle influences the fluid field little.

4. Discussion and conclusion

Figs. 2 and 3 numerically described the induced pressure for diffuser angles of 30° and 60° at steady state. The pressure near wall in diffuser is larger than that in upstream. High negative pressure gradient hinders power-law fluids from decreasing the velocity in diffuser. This is why Fig. 4(b) and (c) show that the axially velocity gradient without pressure gradient is more obvious than that with pressure gradient. When section is various for the diffuser angle not equal to 0° , three kinds of fluids all have the larger errors and errors that increase with the value of diffuser angle. That is verified in Fig. 4.

This paper mainly studies the induced pressure field in EOF at steady state while diffuser angles are 30° and 60° . Results show that the velocity with induced pressure gradient has great difference from the velocity without it. And the influence of induced pressure gradient should be considered in researches about smaller viscosity such as the shear thinning fluid. Because the error of velocity for shear thinning fluid with induced pressure gradient is the largest. If the section is various, the induced pressure gradient of power-law fluids cannot be omitted.

Acknowledgements

Project supported by the Major Research Plan of the National Natural Science Foundation of China (Grant No. 91230114).

References

- [1] G. H. Tang, X. F. Li, Y. L. He, Electroosmotic flow of non-Newtonian fluid in microchannels, *Journal of Non-Newtonian Fluid Mechanics*. 133(2009) 133-137.
- [2] C. L. Zhao, C. Yang, An exact solution for electroosmosis of non-Newtonian fluids in microchannels, *Journal of Non-Newtonian Fluid Mechanics*. 166(2011) 1076-1079.
- [3] Y. H. Zhang, X. J. Gu, R. W. Barber, D. R. Emerson, An analysis of induced pressure fields in electroosmotic flows through microchannels, *Journal of Colloid and Interface Science*. 275(2004) 670-678.
- [4] L. Chen, A. T. Conlisk, Electroosmotic flow and particle transport in micro/nano nozzles and diffusers, *Biomed Microdevices*. 10(2008) 289-298.
- [5] Y. J. Kang, C. Yang, X. Y. Huang, Dynamic aspects of electroosmotic flow in a cylindrical microcapillary, *International Journal of Engineering Science*. 40(2002) 2203-2221.
- [6] Q. Y. Zhu, S. Y. Deng, Y. Q. Chen, Periodical pressure-driven electrokinetic flow of power-law fluids through a rectangular microchannel, *Journal of Non-Newtonian Fluid Mechanics*. 203(2014) 38-50.